Author(s): Puttreddy, Rakesh; von Essen, Carolina; Rissanen, Kari

Title: Halogen Bonds in Square Planar 2,5-Dihalopyridine-Copper(II) Bromide Complexes

Please cite the original version:

Puttreddy, R., von Essen, C., & Rissanen, K. (2018). Halogen Bonds in Square Planar 2,5-
Dihalopyridine-Copper(II) Bromide Complexes. European Journal of Inorganic Chemistry,
2018(20-21), 2393-2398. https://doi.org/10.1002/ejic.201800144

Accepted Article

WILEY-VCH

FULL PAPER

Halogen Bonds in Square Planar 2,5-Dihalopyridine-Copper(II) Bromide Complexes

Rakesh Puttreddy,[a] Carolina von Essen,[a] and Kari Rissanen*[a]

Dedication ((optional))

Abstract: Halogen bonding in self-complementary 1:2 metal-ligand complexes obtained from copper(II) bromide ($CuBr_2$) and seven 2,5-dihalopyridines are analyzed using single crystal X-ray diffraction. All presented discrete complexes form 1-D polymeric chains connected with C–X···Br–Cu halogen bonds (XB). In (2-chloro-5-X-pyridine)$_2$·$CuBr_2$ (X = Cl, Br and I), only the C5-halogen, and in (2-bromo-5-X-pyridine)$_2$·$CuBr_2$ (X = Cl, Br and I) both, C2- and C5-halogens, form C–X···Br–Cu halogen bonds with the X acting as the XB donor and copper-coordinated bromide as the XB acceptor. The electron withdrawing C2-chloride in 2-chloro-5-X-pyridine-$CuBr_2$ complexes has only a minor effect on the C5–X5···Br–Cu XBs, and the X5···Br distances follow expected order, I5 < Br5 < Cl5 in the R_{XB} values of 0.91, 0.94 and 0.99, respectively. In 2-bromo-5-X-pyridine-$CuBr_2$ complexes, due to the polarization of both halogens, the C2–X2···Br–Cu and C5-X5···Br–Cu the R_{XB} values are very similar [0.92 – 0.99] due to competition of C2- and C5-halogens for XB formation. In addition to the classical halogen bonds the square planar Cu(II) complexes exhibit C2–X2···Cu (X = Cl and Br) contacts perpendicular to the Br–Cu–Br plane with shorter C2–Br2···Cu than C2–Cl2···Cu contacts. These interactions induce a *pseudo*-octahedral geometry for Cu(II) ions. Notably, C2–X2···Br–Cu halogen bonds and the additional C2–X2···Cu contacts are slightly enhanced by the C5-halogen electronegativity.

Introduction

The importance of hydrogen bonds[1] (HB) in organic, organometallic and inorganic compounds has led to significant interest to other non-covalent interactions, most recently to the utilization of halogen bonding. The halogen bonds (XB), are predominantly studied in organic molecules and in the solid-state, as strong, specific and highly directional non-covalent interactions equivalent to HBs resulting in a rapidly developing area within supramolecular chemistry.[2] Over the past decade, C–X···A–C [C = carbon, X = halogen as XB donor, A = XB acceptor, often halide anion], halogen bonding interactions have been of growing interest as valuable crystal engineering tool.[3] The halogen bond has recently been defined[4] by IUPAC and has recently been

extensively studied,[2-3] also for complex halide anions[5] using solid-state X-ray crystallography and computational methods.[2-6] In transition metal complexes, the importance and the role of two descriptors are well studied, *viz.*, (a) primary coordination sphere or metal-ligand interactions, and (b) secondary coordination sphere or non-covalent interactions.[7] Structure and reactivity of metal complexes depend on metal-ligand interactions, while most chemical and physical properties are influenced by non-covalent interactions, *e.g.* HB and XB. In the solid-state X-ray crystal structures, the functional groups attached to the ligands in the coordination complexes gives rise to rich chemical environments allowing for variety of intra- and intermolecular non-covalent interactions from the substituents. To investigate XBs in metal complexes, halopyridines coordinated to metal ions makes it possible to study both C–X···A–C and C–X···A–M [X = halogen substituent, M = metal ion, A = XB acceptor] interactions. A few research groups, mainly, Brammer *et al.*,[8] have crystallographically studied complexes of the type M(LX)$_2$A$_2$ [LX = 2-, 3- and 4-halopyridines, M = metal and A = metal bound halides], where A acts as XB acceptor and X as XB donor. Furthermore, Brammer *et al.* explored the cooperative and competitive nature of HBs and XBs of [LH]$^+$ species as acceptors to tetrahedral MA$_4$ anions.[9] To complement this, we have previously studied neutral pincer type *viz.*, {2,6-bis[(di-*t*-butylphosphino)-methyl]phenyl}PdY (Y = Cl, Br and I) and (terpyridine)Me$_3$PtI complexes where the metal bound halogen acts as the XB acceptor.[10]
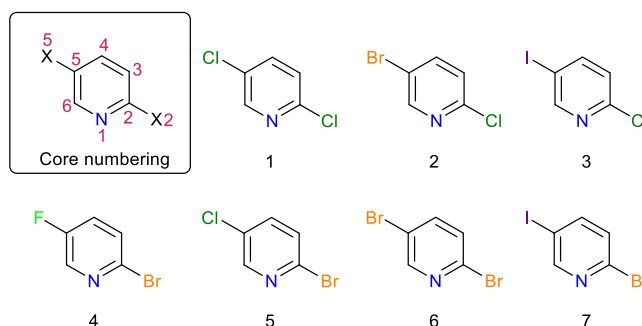

Figure 1. Representation of 2,5-dihalopyridine core numbering, and chemical structures of 2,5-dichloropyridine (**1**), 5-bromo-2-chloropyridine (**2**), 2-chloro-5-iodopyridine (**3**), 2-bromo-5-fluoropyridine (**4**), 2-bromo-5-chloropyridine (**5**), 2,5-dibromopyridine (**6**) and 2-bromo-5-iodopyridine (**7**).

In the present study, we analyze the halogen bonds in coordination complexes formed from 2,5-dihalopyridines and copper(II) bromide ($CuBr_2$). We utilize a series of seven 2,5-dihalopyridines, three based on 2-chloropyridine (**1-3**) and four based on 2-bromopyridine (**5-7**), with a different halogen substituent at the 5-position of the pyridine ring [X5, Fig. 1]. We anticipated that, upon complexation with $CuBr_2$, the X5

[a]   Rakesh Puttreddy, Carolina von Essen and Kari Rissanen
       University of Jyvaskyla, Department of Chemistry, P.O. Box. 35,
       40014 Jyväskylä, Finland
       E-mail: rakesh.r.puttreddy@jyu.fi and kari.t.rissanen@jyu.fi
       https://www.jyu.fi/science/en/chemistry/research/structural-and-synthetic-chemistry/the-supramolecular-chemistry

       Supporting information for this article is given via a link at the end of the document.

FULL PAPER

substituent will be electronically influenced by the X2 substituent as it resides close to positive Cu(II) coordination sphere. The formally negatively-charged bromide atoms bound to the Cu(II) ion are nucleophilic enough to act as the XB acceptors. However, considering different coordination geometries of Cu(II) and the orientation of ligands influenced by crystal packing interactions, this study further aims to examine: (a) whether either X2 or X5 or both of them are able to form C–X···Br–Cu halogen bonds in the solid-state. The crystallographic studies are supplemented by qualitative analysis of the electrostatic potential surfaces of the complexes, *viz.* by visualizing the modulation of the σ-hole at the X2 or X5 substituent or *vice versa*. In the following discussion, 2-chloro-, 2-bromo-, 3-chloro- and 3-bromopyridines from the literature[11] are abbreviated as 2ClPy, 2BrPy, 3ClPy and 3BrPy.

Results and Discussion

The complexes were synthesized by mixing a 2:1 molar ratio of 2,5-dihalopyridine and $CuBr_2$ in acetonitrile at room temperature. If necessary, the reaction mixtures were sonicated to dissolve all the components. Slow evaporation of the resulting solution provides single crystals suitable for X-ray crystallography (See Experimental Section for more details). Attempts to obtain crystals with 2-chloro-5-fluoropyridine were unsuccessful. In all complexes, the Cu(II) ion binds to two 2,5-dihalopyridine ligands and has centrosymmetric N_2Br_2 coordination sphere. In complexes $(1)_2 \cdot CuBr_2$ and $(2)_2 \cdot CuBr_2$, Cu(II) is square planar, while $(3)_2 \cdot CuBr_2$ has see-saw geometry with an τ_4 value of 0.47.[12] In contrast to the reported square planar structure, (2-ClPy)$_2 \cdot CuBr_2$ (CCDC code PAMLEW),[11a] the C2-chlorides in $(1)_2 \cdot CuBr_2$ and $(2)_2 \cdot CuBr_2$ are in *anti*-arrangement. However, the *anti*-arrangement of X5 substituent in $(1)_2 \cdot CuBr_2$ and $(2)_2 \cdot CuBr_2$ is similar to (3-ClPy)$_2 \cdot CuBr_2$ (CCDC code PAMKUL)[11a] and (3-BrPy)$_2 \cdot CuBr_2$ (CCDC code YENXUL).[11b] The small energy difference between *syn*- and *anti*-arrangements of the Cl2 substituents are reported,[11a] the C2-Cl2···Cu contacts, particularly in *anti*-positions play a crucial role to stabilize square planar rather than distorted four coordinate Cu(II) geometries. The *trans*-C2-Cl2···Cu contacts of 3.0 Å around Cu(II) ion in $(1)_2 \cdot CuBr_2$ and $(2)_2 \cdot CuBr_2$ are remarkably short, *ca*. 3.04 Å, while

the distance of *ca*. 3.12 Å around see-saw geometry Cu(II) ion in $(3)_2 \cdot CuBr_2$ is similar to reported (2ClPy)$_2 \cdot CuBr_2$ [Fig. 2d].[11a]
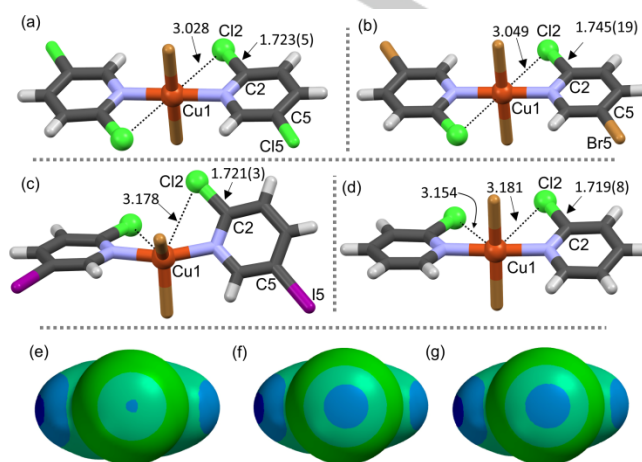
Figure 2. X-ray crystal structure of (a) $(1)_2 \cdot CuBr_2$, (b) $(2)_2 \cdot CuBr_2$, (c) and $(3)_2 \cdot CuBr_2$ compared with the previously reported[11a] structure of (d) (2ClPy)$_2 \cdot CuBr_2$. The electrostatic potential surfaces of X5 in free ligands (e) for **1** (Cl), (f) for **2** (Br) and (g) for **3** (I).

Complexes $(1)_2 \cdot CuBr_2$ and $(2)_2 \cdot CuBr_2$ are isomorphous and isostructural, and $(3)_2 \cdot CuBr_2$ is remarkably different in both crystallographic cell parameters as well as from structural perspective. The discrete metal complexes are extended to 1-D polymers *via* C5–X5···Br–Cu (X = Cl, Br and I) halogen bonds, as shown in Fig. 3 and Table 1. The C2-chlorides in $(1)_2 \cdot CuBr_2$ and $(2)_2 \cdot CuBr_2$ are not showing halogen bonding. The C5–Cl5···Br–Cu and C5–Br5···Br–Cu halogen bonds in $(1)_2 \cdot CuBr_2$ [$R_{XB} = 0.99$] and $(2)_2 \cdot CuBr_2$ [$R_{XB} = 0.94$] are stronger when compared to C3–X3···Br–Cu distances observed in (3-ClPy)$_2 \cdot CuBr_2$ [$R_{XB} = 1.02$][11a] and (3-BrPy)$_2 \cdot CuBr_2$ [$R_{XB} = 0.98$] [11b], respectively. This suggests that the electron withdrawing Cl2-substituent *para* to X5 increase the electrophilic character of X5 resulting in shorter C5–X5···Br–Cu contacts. Despite the Cl2 being XB passive in $(1)_2 \cdot CuBr_2$ and $(2)_2 \cdot CuBr_2$, the 1-D chains are connected *via* weak C2–Cl2···H–C3 HB interactions to form a 3-D crystal lattice [See ESI, Fig. S1a].

Table 1. Solid-state X-ray crystallography bond parameters^a for complexes $(1)_2 \cdot CuBr_2$ - $(7)_2 \cdot CuBr_2$.

Complex	Motif	d (X2···Br), Å	∠C2–X2···Br (°)	R_{XB}^b	Motif	d (X5···Br), Å	∠C5–X5···Br (°)	R_{XB}^b
$(1)_2 \cdot CuBr_2$	C2–Cl2···Br–Cu	3.70^c	159.2^c	1.03^c	C5–Cl5···Br–Cu	3.546 [3.661]	170.6 [162.2]	0.99 [1.02]
$(2)_2 \cdot CuBr_2$	C2–Cl2···Br–Cu	3.727^c	159.3^c	1.04^c	C5–Br5···Br–Cu	3.489 [3.624]	173.1 [161.1]	0.94 [0.98]
$(3)_2 \cdot CuBr_2$	C2–Cl2···Br–Cu	3.603^c	161.0^c	1.00^c	C5–I5···Br–Cu	3.478 [3.506]^d	174.2 [170.9]^d	0.91 [0.92]^d
$(4)_2 \cdot CuBr_2$	C2–Br2···Br–Cu	3.492 [3.460]	163.7 [163.4]	0.94 [0.94]	C5–F5···Br–Cu	3.741^e	161.3^e	1.13^e
$(5)_2 \cdot CuBr_2$	C2–Br2···Br–Cu	3.544 [3.460]	163.9 [163.4]	0.96 [0.94]	C5–Cl5···Br–Cu	3.550 [3.661]	171.2 [162.2]	0.99 [1.02]
$(6)_2 \cdot CuBr_2$	C2–Br2···Br–Cu	3.565 [3.460]	165.0 [163.4]	0.96 [0.94]	C5–Br5···Br–Cu	3.507 [3.624]	172.6 [161.1]	0.95 [0.98]
$(7)_2 \cdot CuBr_2$	C2–Br2···Br–Cu	3.531 [3.460]	168.0 [163.4]	0.95 [0.94]	C5–I5···Br–Cu	3.523 [3.506]	173.2 [170.9]	0.92 [0.92]

^{a}The values in parentheses are C2- and C3-halogen based XB bond parameters in mono-substituted halopyridine-$CuBr_2$ complexes extracted from CSD database[13]; ^{b}The normalized interaction ratio, R_{XB}, is defined as $(R_{XB} = d_{XB}/X_{vdw}+B_{vdw})$,[14] where d_{XB} [Å] is the distance between the donor atom (X) and the acceptor atoms (B) and divided by the sum of vdW radii [Å] of X and B. The van der Waals radii determined by Bondi were used to calculate R_{XB} values.[15]; ^{c}The values are only for reference purpose and no C2–Cl2···Br–Cu XBs were observed; ^{d}Part of current study, see supporting information Fig S2 for X-ray crystal structure; ^{e}For comparison, crystal structure not available for (3-fluoropyridine)$_2 \cdot CuBr_2$.

FULL PAPER

In (3)$_2$·CuBr$_2$, the distorted Cu(II) geometry and the relative *syn*-positions of bromides bound to Cu(II) ion and I5 of **3** favour 1-D polymeric zig-zag structure [Fig. 3c] through C5–I5···Br–Cu halogen bonds [R$_{XB}$ = 0.91]. A closer inspection of crystal packing in (3)$_2$·CuBr$_2$, reveals also weak C2–Cl2···Br–Cu contacts between adjacent 1-D chains [See ESI, Fig. S1b]. Thus, the order of XB strength increases in the order: (1)$_2$·CuBr$_2$ < (2)$_2$·CuBr$_2$ < (3)$_2$·CuBr$_2$ according to the electrophilic character of the halogens[6c] *i.e.*, Cl5<Br5<I5 [Fig. 2e-g].
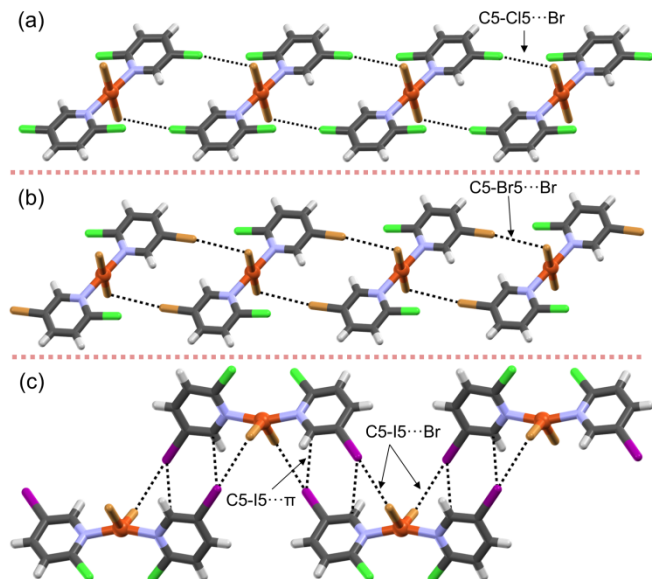

Figure 3. Section of crystal packing to display the 1-D halogen bonded polymeric structures in (a) (1)$_2$·CuBr$_2$, (b) (2)$_2$·CuBr$_2$ and (c) (3)$_2$·CuBr$_2$. The halogen bonds are shown in black dotted lines.

The 2BrPy in the previously published (2-BrPy)$_2$·CuCl$_2$ complex can be regarded as chelating rather than mono-dentate ligand, and Cu(II) ion as octahedral rather than square planar.[16] The report[16] reasoned that, the unusually short C2–Br2···Cu distance between the *ortho*-bromide and square planar Cu(II) ion results in a *pseudo*-octahedral N$_2$Cl$_2$Br$_2$ coordination sphere. In fact, the role of C2–X···Cu type interactions were overlooked in solid-state chemistry, although they are important to stabilize both metals and coordination polymers. The X-ray crystal structures of (4)$_2$·CuBr$_2$, (5)$_2$·CuBr$_2$, (6)$_2$·CuBr$_2$ and (7)$_2$·CuBr$_2$ all contain square planar Cu(II) ions, and exhibit C2–Br2···Cu interactions as shown in Fig. 4. The increase in size of the X2, Cl to Br, increases the possibility to X2···Cu interactions, and makes it a significant synthon of interest. Such systems have been studied using computational methods and X-ray crystal structures by Awwadi *et al*.[16] The electrostatic negative potential around X2 interacts with the electrophile *i.e.*, Cu(II) ion. Halogens F, Cl, Br and I positioned *para* to the Br2 have an influence to the C2–Br2···Cu interaction, as shown in Fig. 4. Our results show that the higher the electronegativity of the X5 is, the shorter the shorter the C2–Br2···Cu interaction distances. The C2–Br2···Cu contacts of 3.074 Å in (4)$_2$·CuBr$_2$ is similar to distances observed in (2BrPy)$_2$·CuBr$_2$ [3.071 Å].[11b]
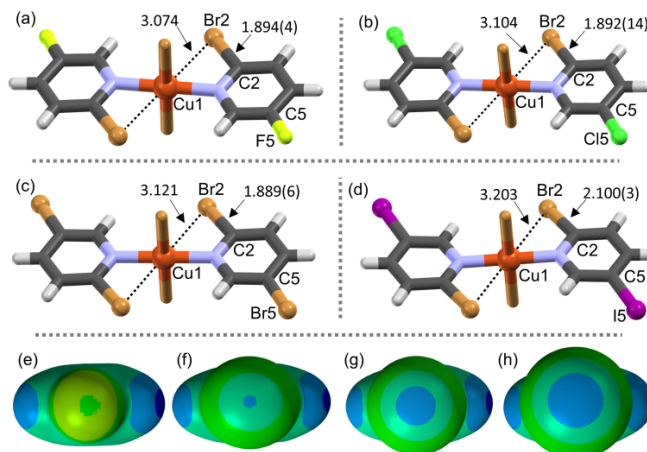
Figure 4. X-ray Crystal structures of (a) (4)$_2$·CuBr$_2$, (b) (5)$_2$·CuBr$_2$, (c) (6)$_2$·CuBr$_2$ and (d) (7)$_2$·CuBr$_2$ to display *pseudo*-octahedral Cu(II) ion with N2Br4 coordination sphere. The electrostatic potential surfaces of the X5 of the free ligands are shown in (e) for **4** (F), (f) for **5** (Cl), (g) for **6** (Br) and (h) for **7** (I).

Complexes (4)$_2$·CuBr$_2$, (5)$_2$·CuBr$_2$ and (6)$_2$·CuBr$_2$, crystallize in the triclinic space group *P*-1, are isomorphous and isostructural, while (7)$_2$·CuBr$_2$ crystallizes in monoclinic space group *P*2$_1$/*n* and packs with a herringbone pattern. The structure of (6)$_2$·CuBr$_2$ is similar to previously reported (CCDC code XIBSAE).[17] The formation of 1-D polymers in (4)$_2$/(5)$_2$/(6)$_2$/(7)$_2$·CuBr$_2$ is due to interactions between the Br2 and Br–Cu instead of X5 as observed in (1)$_2$/(2)$_2$/(3)$_2$·CuBr$_2$ structures. The C2–Br2···Br–Cu XBs in (4)$_2$/(5)$_2$/(6)$_2$/(7)$_2$·CuBr$_2$ have R$_{XB}$'s 0.94, 0.96, 0.96 and 0.95, respectively. The C5–X5···Br–Cu (X = Cl, Br and I) halogen bonded 1-D polymers in (5)$_2$/(6)$_2$/(7)$_2$·CuBr$_2$ are interconnected with secondary weak XBs between the Br2 and the adjacent polymer Br–Cu, extending the polymers into 2-D network as shown in Fig. 5a-c. The X5···Br halogen bond distances with R$_{XB}$'s 0.99, 0.95 and 0.92 are longer than the corresponding values observed in (1)$_2$/(2)$_2$/(3)$_2$·CuBr$_2$ complexes. The C5–F5···Br–Cu distances in (4)$_2$·CuBr$_2$ are above the sum of the vdW radii [3.32 Å], and cannot be regarded as halogen bonds. However, their relative positioning in the crystal lattice is caused due to favourable electrostatic interactions. To rationalize C–X···Br–Cu contacts, X-ray crystal structure coordinates of 1:2 metal-ligand complexes were used to calculate electrostatic potential surfaces for the X2- and X5 substituents [see ESI].[18] The X2 and X5 substituents, notably chlorides, in modelled free ligands [Fig. 2 and 4] show more pronounced positive potential compared to Cu(II) complexes [see ESI, Fig. S3-S9].

Non-covalent electrostatic interactions can either be strong or act at long range, and are overlooked due to difficulty in visualizing clear surface potentials. The isostructural packing in (4)$_2$·CuBr$_2$, (5)$_2$·CuBr$_2$ and (6)$_2$·CuBr$_2$, can be used to view ligand alignments for short and long range contacts. In (4)$_2$·CuBr$_2$, the formally negatively charged bromide of Cu–Br and aromatic C5-carbon of C5-F5 exhibit Cu–Br···C(π) contacts with R$_{XB}$ = 0.98 [3.485 Å]. The halogen···C(π) interaction in (4)$_2$·CuBr$_2$, and similarly short contacts observed in other

FULL PAPER
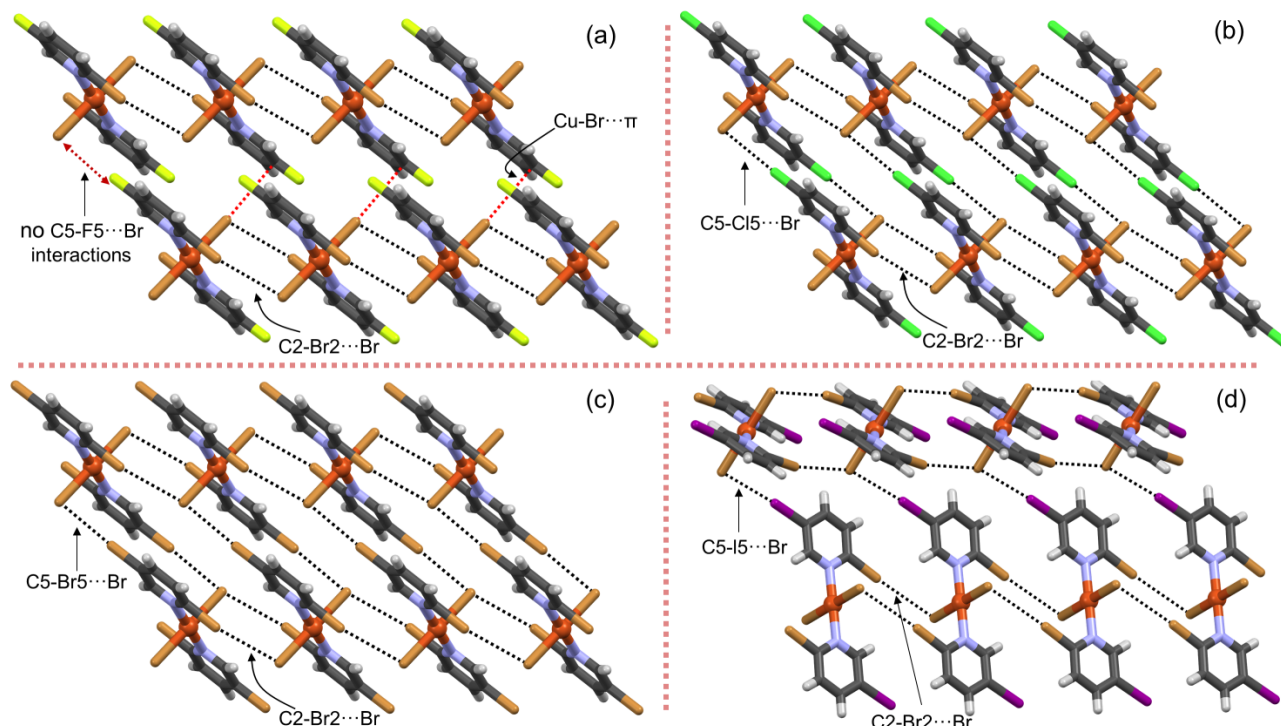
Figure 5. Perspective view of one dimensional halogen bonded polymers in (a) (**4**)$_2$·CuBr$_2$, (b) (**5**)$_2$·CuBr$_2$, (c) (**6**)$_2$·CuBr$_2$ and (d) (**7**)$_2$·CuBr$_2$. The black dotted lines represent the halogen bonds.

structures were analysed using Hirshfeld surfaces.[19] The red-hot spots as an indication of short contacts between halogens and π-carbons were depicted in Fig. S10 [See Supporting Information]. The C2–X2···Br–Cu and C5–X5···Br–Cu XB distances are dependent on electronegativity of X2 and X5 substituents. For example, the more electronegative Cl2 in (**1**)$_2$·CuBr$_2$, (**2**)$_2$·CuBr$_2$ and (**3**)$_2$·CuBr$_2$ causes shortening of C5–X5···Br–Cu distances by electron-withdrawing effect. Similar behaviour can be observed in (**4**)$_2$·CuBr$_2$, *i.e.*, the more electronegative F5 shortens C2–X2···Br–Cu contacts. The C2–X2···Br–Cu and C5–X5···Br–Cu XB distances in (**5**)$_2$·CuBr$_2$, (**6**)$_2$·CuBr$_2$ and (**7**)$_2$·CuBr$_2$ are similar, due to relatively similar electronegativity of X2 and X5 substituents and simultaneous competition for halogen bonds. This further explains the longer C2–Br2···Br–Cu distances in (**5**)$_2$·CuBr$_2$ [R$_{XB}$ = 0.96] compared to (2-BrPy)$_2$·CuBr$_2$ [R$_{XB}$ = 0.94] despite the more electronegative Cl5. In contrast, the more electronegative Cl2 has a significant influence on C5–Br5···Br–Cu XBs in (**4**)$_2$·CuBr$_2$.

complexes form 1-D polymer chains through halogen bonds between the halogen X2 or X5 substituent (donor) and copper-bound bromide anion (acceptor). In (2-chloro-5-halopyridine)$_2$·CuBr$_2$ complexes, only X5 forms halogen bonds. However, in (2-bromo-5-halopyridine)$_2$·CuBr$_2$ both X2 and X5 substituents form C–X···Br–Cu halogen bonds. The more electronegative F5 in (2-bromo-5-fluoropyridine)$_2$·CuBr$_2$ is XB passive but polarizes the Br2 to form Br2···Br–Cu halogen bonds. The C5–X5···Br–Cu halogen bond angles for the (2,5-dihalopyridine)$_2$·CuBr$_2$ complexes are closer to 180° when compared to the previously reported C3–X3···Br–Cu in (3-halopyridine)$_2$·CuBr$_2$ complexes. The C2–X2···Br–Cu and C5–X5···Br–Cu halogen bonds are of similar strength in (2-bromo-5-halopyridine)$_2$·CuBr$_2$ complexes due to competition of both X2 and X5 for halogen bonds. All complexes exhibit pseudo-octahedral C2–X2···Cu contacts, with stronger interactions for bromide than for chloride.

Conclusions

The modulation of the C–X···Br–Cu halogen bonds and C–X···Cu interactions using a series of 2,5-dihalopyridines have been demonstrated in 2,5-dihalopyridine-copper(II) bromide complexes. Compared to previously published mono-substituted halopyridines, the di-substituted halopyridines have been proven to act as better synthons to understanding the electronic donor-acceptor properties in solid-state. The discrete 1:2 metal-ligand

Experimental Section

FULL PAPER

General crystallization procedure: To a solution of CuBr$_2$ (0.067 mmol) in acetonitrile (1.0 ml), was added respective 2,5-dihalopyridine (0.134 mmol) dissolved in acetonitrile (0.5 ml) at room temperature. In case of precipitation, the samples were sonicated to clear solutions. The solutions were left in dark at room temperature, and subjected to slow evaporation to give single crystals suitable for X-ray diffraction analysis.

(**1**)$_2$·CuBr$_2$: IR v_{max} cm^{-1}: 3070, 2918, 2552, 1678, 1581, 1452, 1417, 1323, 1286, 1180, 1100, 913, 803, 702, 664, 542, 430.

(**2**)$_2$·CuBr$_2$: IR v_{max} cm^{-1}: 3088, 1549, 1450, 1410, 1357, 1233, 1109, 1096, 1042, 912, 827, 717, 661, 516, 498, 438.

(**3**)$_2$·CuBr$_2$: IR v_{max} cm^{-1}: 3082, 1558, 1443, 1346, 1130, 1021, 906, 817, 715, 643, 493, 483, 414.

(**4**)$_2$·CuBr$_2$: IR v_{max} cm^{-1}: 3088, 2388, 1578, 1456, 1373, 1267, 1229, 1097, 1031, 832, 711, 601, 528, 439, 430.

(**5**)$_2$·CuBr$_2$: IR v_{max} cm^{-1}: 3030, 1575, 1468, 1436, 1397, 1358, 1271, 1127, 1109, 1086, 1003, 913, 829, 754, 716, 624, 484.

(**6**)$_2$·CuBr$_2$: IR v_{max} cm^{-1}: 3086, 1569, 1466, 1401, 1354, 1278, 1231, 1124, 1101, 1085, 1041, 907, 827, 754, 713, 659, 495, 435.

(**7**)$_2$·CuBr$_2$: IR v_{max} cm^{-1}: 3078, 1557, 1438, 1384, 1343, 1279, 1217, 1133, 1095, 1073, 1040, 1017, 904, 815, 708, 659, 640, 477, 409.

(3IPy)$_2$·CuBr$_2$: IR v_{max} cm^{-1}: 3052, 1584, 1460, 1417, 1407, 1324, 1223, 1193, 1120, 1042, 1030, 915, 790, 685, 648, 527, 450, 409.

Crystal structure determination: The X-ray single crystal data and experimental details for data collections are given in Supporting Information Table S1 and S2. Single-crystal X-ray data for (**1**)$_2$·CuBr$_2$, (**2**)$_2$·CuBr$_2$, (**3**)$_2$·CuBr$_2$, (**4**)$_2$·CuBr$_2$, (**5**)$_2$·CuBr$_2$, (**6**)$_2$·CuBr$_2$ and (**7**)$_2$·CuBr$_2$, were measured on a Bruker-Nonius Kappa CCD diffractometer equipped with an APEX-II CCD detector using graphite-monochromated Mo-Kα (λ = 0.71073 Å) radiation. The data for (3IPy)$_2$·CuBr$_2$ was measured at 120.0 K using a Rigaku SuperNova dual-source Oxford diffractometer equipped with an Atlas detector using mirror-monochromated Cu-Kα (λ = 1.54184 Å) radiation. The data collection and reduction for (3IPy)$_2$·CuBr$_2$ were performed using the program *CrysAlisPro*.[20] For the data obtained from Bruker Nonius Kappa diffractometer were performed using the program COLLECT[21] and HKL DENZO AND SCALEPACK.[22] The gaussian face index absorption correction method[20] was used for (3IPy)$_2$·CuBr$_2$. The intensities for data collected using Bruker Nonius Kappa diffractometer were corrected for absorption using SADABS[23] with multi-scan absorption correction type method. All structures were solved with direct methods (*SHELXS*)[24] and refined by full-matrix least squares on F^2 using the *OLEX2* software[25], which utilizes the *SHELXL*-2013 module.[24]

Acknowledgements

[1] (a) G. A. Jeffrey, *An Introduction to Hydrogen Bonding*, Oxford University Press, New York and Oxford, **1997**; (b) G. R. Desiraju, T. Steiner, *The Weak Hydrogen Bond: In Structural Chemistry and Biology*, International union of Crystallography, Monographs on Crystallography, Oxford University Press, Oxford and New York, **2001**; (c) G. Gilli, P. Gilli, *The Nature of the Hydrogen Bond: Outline of a Comprehensive Hydrogen Bond Theory*, OUP Oxford, New York, **2009**; (d) I. Haiduc, F. T. Edelmann, *Supramolecular Organometallic Chemistry*, Wiley-VCH, Weinheim, **2008**.

[2] (a) L. C. Gilday, S. W. Robinson, T. A. Barendt, M. J. Langton, B. R. Mullaney, P. D. Beer, *Chem. Rev.* **2015**, *115*, 7118–7195; (b) H. Wang, W. Wang, W. J. Jin, *Chem. Rev.* **2016**, *116*, 5072–5104. (c) G. Cavallo, P. Metrangolo, R. Milani, T. Pilati, A. Priimagi, G. Resnati, G. Terraneo, *Chem. Rev.* **2016**, *116*, 2478–2601;

[3] (a) A. M. Maharramov, K. T. Mahmudov, M. N. Kopylovich, A. J. L. Pombeiro, Non-Covalent Interactions in the Synthesis and Design of New Compounds, Wiley-VCH, **2016**. (b) Troff, R. W.; Mäkelä, T.; Topić, F.; Valkonen, A.; Raatikainen, K.; Rissanen, K. Eur. J. Org. Chem. **2013**, 2013, 1617−1637. 456. (c) Rissanen, K. CrystEngComm **2008**, 10, 1107−1113. 457, (d) L. Brammer, Chem. Soc. Rev. **2004**, 33, 476–489.

[4] (a) G. R. Desiraju, P. S. Ho, L. Ko, A. C. Legon, R. Marquardt, P. Metrangolo, P. Politzer, G. Resnati and K. Rissanen, *Pure Appl. Chem.* **2013**, *85*, 1711; (b) P. Metrangolo, G. Resnati, *IUCrJ*, **2014**, *1*, 5–7.

[5] (a) P. Metrangolo, Y. Carcenac, M. Lahtinen, T. Pilati, K. Rissanen, A. Vij and G. Resnati, *Science,* **2009**, 323, 1461–1464; (b) A. Abate, M. Brischetto, G. Cavallo, M. Lahtinen, P. Metrangolo, T. Pilati, S. Radice, G. Resnati, K. Rissanen and G. Terraneo, *Chem. Commun.,* **2010**, 46, 2724–2726; (c) M. Müller, M. Albrecht, V. Gossen, T. Peters, A. Hoffmann, G. Raabe, A. Valkonen and K. Rissanen, Chem. Eur. J, **2010**, 16, 12446-12453.

[6] (a) M. H. Kolář, P. Hobza, *Chem. Rev.* **2016**, *116*, 5155–5187 (*reference therein*); (b) F. F. Awwadi, R. D. Willett, K. A. Peterson, B. Twamley, *Chem. – A Eur. J.* **2006**, *12*, 8952–8960 (*reference therein*); (c) K. Riley, J. Murray, J. Fanfrlík, J. Řezáč, R. Solá, M. Concha, F. Ramos, P. Politzer, *J. Mol. Model.* **2011**, *17*, 3309–3318; (d) P. Politzer, J. S. Murray, *ChemPhysChem* **2013**, *14*, 278–294; (e) P. Politzer, J. S. Murray, T. Clark, *Phys. Chem. Chem. Phys.* **2013**, *15*, 11178–11189; (f) P. Politzer, J. S. Murray, T. Clark, *Phys. Chem. Chem. Phys.* **2013**, *15*, 11178–11189; (g) T. Clark, P. Politzer, J. S. Murray, *Wiley Interdiscip. Rev. Comput. Mol. Sci.* **2015**, *5*, 169–177; (h) P. Politzer, K. E. Riley, F. A. Bulat, J. S. Murray, *Comput. Theor. Chem.* **2012**, *998*, 2–8.

[7] (a) R. L. Shook, A. S. Borovik, *Inorg. Chem.* **2010**, *49*, 3646–3660 (*reference therein*); (b) S. A. Cook, A. S. Borovik, *Acc. Chem. Res.* **2015**, *48*, 2407–2414 .

[8] (a) F. Zordan, L. Brammer, P. Sherwood, *J. Am. Chem. Soc.* **2005**, *127*, 5979–5989; (b) F. Zordan, L. Brammer, *Cryst. Growth Des.* **2006**, *6*, 1374–1379.

[9] (a) F. Zordan, S. L. Purver, H. Adams, L. Brammer, *CrystEngComm* **2005**, *7*, 350–354; (b) L. Brammer, G. Minguez Espallargas, H. Adams, *CrystEngComm* **2003**, *5*, 343–345; (c) G. Mínguez Espallargas, L. Brammer, P. Sherwood, *Angew. Chemie Int. Ed.* **2006**, *45*, 435–440.

[10] (a) M. T. Johnson, Z. Džolić, M. Cetina, O. F. Wendt, L. Öhrström, K. Rissanen, *Cryst. Growth Des.* **2012**, *12*, 362–368; (b) B. N. Ghosh, M. Lahtinen, E. Kalenius, P. Mal, K. Rissanen, *Cryst. Growth Des.* **2016**, *16*, 2527–2534.

[11] (a) F. Awwadi, R. D. Willett, B. Twamley, *Cryst. Growth Des.* **2011**, *11*, 5316–5323; (b) F. Awwadi, R. D. Willett, S. F. Haddad, B. Twamley, *Cryst. Growth Des.* **2006**, *6*, 1833–1838.

[12] L. Yang, D. R. Powell, R. P. Houser, *Dalton Trans.* **2007**, 955–964

[13] (a) The Cambridge Structural database 2018 [updated December 2017], ConQuest version 1.19; (b) I. J. Bruno, J. C. Cole, P. R. Edgington, M. Kessler, C. F. Macrae, P. McCabe, J. Pearson, R. Taylor, *Acta Crystallogr. Sect. B* **2002**, *58*, 389–397.

[14] R. Puttreddy, O. Jurček, S. Bhowmik, T. Mäkelä, K. Rissanen, *Chem. Commun.* **2016**, *52*, 2338–2341.

[15] A. Bondi, *J. Phys. Chem.* **1964**, *68*, 441–451

[16] F. F. Awwadi, R. D. Willett, B. Twamley, M. M. Turnbull, C. P. Landee, *Cryst. Growth Des.* **2015**, *15*, 3746–3754.

[17] F. F. Awwadi, S. F. Haddad, M. M. Turnbull, C. P. Landee, R. D. Willett, *CrystEngComm* **2013**, *15*, 3111–3118.

[18] *Spartan'16* (version 2.0.8), Wavefunction, Inc., Irvine, USA..

FULL PAPER

[19] (a) M. A. Spackman, D. Jayatilaka, *CrystEngComm* **2009**, *11*, 19–32; (b) J. J. McKinnon, M. A. Spackman, A. S. Mitchell, *Acta Crystallogr. Sect. B* **2004**, *60*, 627–668; (c) M. A. Spackman, J. J. McKinnon, D. Jayatilaka, *CrystEngComm* **2008**, *10*, 377–388.

[20] *Rigaku Oxford Diffraction 2017*, *CrysAlisPro* Version 1.171.38.43.

[21] Bruker AXS BV, Madison, WI, USA; 1997–2004.

[22] Z. Otwinowski, W. Minor, *Methods Enzymol.* **1997**, 276, 307–326.

[23] R. H. Blessing, *J. Appl. Cryst.* **1997**, 30, 421–426.

[24] (a) G. M. Sheldrick, *Acta Cryst.* **2008**, A64, 112–122; (b) G. M. Sheldrick, *Acta Cryst.* **2015**, A71, 3-8.

[25] O. V. Dolomanov, L. J. Bourhis, R. J. Gildea, J. A. K. Howard, H. J. Puschmann, *J. Appl. Cryst.* **2009**, 42, 339–341.

FULL PAPER

Entry for the Table of Contents

Layout 2:

FULL PAPER
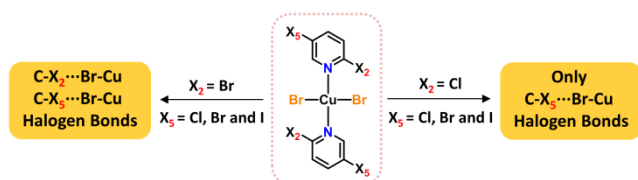
Halogen Bonding

Rakesh Puttreddy*, Carolina von Essen and Kari Rissanen*

Page No. – Page No.

Halogen Bonds in Square Planar 2,5-Dihalopyridine-Copper(II) Bromide Complexes

Table of contents text: 2,5-Dihalopyridine-copper(II) bromide complexes were investigated aiming to understand the mutual polarization of X2 on X5 and *vice versa,* and their effect on C–X2/X5···Br–Cu halogen bond distances in solid-state X-ray crystal structures. In this approach, the change in C–X2/X5···Br–Cu halogen bond distances due to X2-/X5-substituent effects are evaluated by comparing with C–X2/X3···Br–Cu halogen bonds in (2-X-pyridine)$_2$•CuBr$_2$ (X = Cl and Br) and (3-X-pyridine)$_2$•CuBr$_2$ (X = Cl, Br and I) complexes, respectively. Our results reveal, in (2-chloro-5-X-pyridine)$_2$•CuBr$_2$ (X = Cl, Br and I), only the X5, and in (2-bromo-5-X-pyridine)$_2$•CuBr$_2$ (X = Cl, Br and I) both, X2- and X5, form C–X···Br–Cu halogen bonds. Several other interesting results such as predominant square planar Cu(II) centers and unqiue C–X2···Cu interactions are reported as a part of our structure-property study that utilizes C–X···Br–Cu halogen bonds.